Failure modes of composite sandwich beams

E.E. Gdoutos[*]   **I.M. Daniel**[†]

Abstract

A thorough investigation of failure behavior of composite sandwich beams under three- and four-point bending was undertaken. The beams were made of unidirectional carbon/epoxy facings and a PVC closed-cell foam core. The constituent materials were fully characterized and in the case of the foam core, failure envelopes were developed for general two-dimensional states of stress. Various failure modes including facing wrinkling, indentation failure and core failure were observed and compared with analytical predictions. The initiation, propagation and interaction of failure modes depend on the type of loading, constituent material properties and geometrical dimensions.

Keywords: sandwich beams, failure modes, carbon/epoxy facings, foam core, wrinkling, indentation.

1 Introduction

A sandwich structure consists of two external thin, strong, stiff facings bonded to a thick light-weight and weaker core. The core carries the through-the-thickness shear loads, while the facings resist in-plane and bending loads. The high specific strength and specific stiffness of sandwich construction coupled with outstanding thermal and acoustic insulation make it ideal in structural design.

Sandwich beams subjected to bending and shear loads may fail in several ways including tension or compression failure of the facings, shear failure of the core, wrinkling failure of the compression facing, local indentation, debonding of the core/facing interface and global buckling. The initiation of each failure mode should be studied separately and is described by a different failure

[*]School of Engineering Democritus University of Thrace GR-671 00 Xanthi, Greece

[†]Departments of Civil and Mechanical Engineering Northwestern University Evanston, IL 60208, USA

equation. The critical load for failure initiation is the lowest load of all potential failure modes. Following initiation of failure by a specific failure mode, interaction of failure modes may occur and failure could progress by another failure mode.

A substantial amount of work has been performed on the failure of sandwich panels by various failure modes. The authors have reviewed and described failure mode in sandwich beams [1]. Core failure by shear has been studied by Alen [2], Hall and Robson [3] and Zenkert [4]. Tension or compression facing failure in uniaxial stress by yielding or fracturing is reported in the above mentioned references and also in [5,6]. Short-wavelength buckling or wrinkling of the compression facing of sandwich beams subjected to compression or bending has been investigated by Hoff and Mautner [7], Gutierrez and Webber [8], Vonach and Rammerstorfer [9] and Hadi and Matthews [10]. Debonding of the facing from the core may occur during fabrication or due to overloads. This failure mode was studied in terms of the critical strain energy release rate of the interface by Triantafillou and Gibson [11]. The load carrying capacity of debonded sandwich composite specimens subjected to axial compression was determined by Avery III and Sankar [12]. Indentation failure of sandwich construction results from application of highly localized external loads and is associated with local bending of the loaded facing into the core. The problem has been studied by Soden [13] and Shuaeib and Soden [14] using a rigid-perfectly plastic and an elastic-perfectly plastic type foundation model. Failure mode maps for sandwich beams with aluminum facings and rigid polyurethane foam cores in three-point bending were constructed by Triantafillou and Gibson [15].

In the present work the failure modes were investigated in composite sandwich beams under three- and four-point bending. The failure modes observed and studied include indentation failure, core failure and compression facing wrinkling.

2   Materials and specimens

The sandwich beams were fabricated from 8-ply unidirectional carbon/epoxy (AS4/3501-6) facings and a PVC foam core. Uniaxial tensile and compressive tests were conducted in the longitudinal direction in order to obtain relevant constitutive behavior of the facing material. The carbon/epoxy exhibits a characteristic stiffening nonlinearity in tension and softening nonlinearity in compression. Two types of a fully cross-linked PVC closed-cell foams, Divinycell H100 and H250, with densities of 100 and 250 kg/m^3, respectively, were investigated as core materials. Divinycell H100 exhibits nearly isotropic behavior, while Divinycell H250 exhibits pronounced axisymmetric anisotropy with much higher stiffness and strength in the cell direction (3-direction). The material

displays different behavior in tension and compression with tensile strengths much higher than corresponding compressive strengths. The uniaxial stress-strain behavior in tension is nonlinear elastic without any identifiable yield region. In uniaxial compression the material is nearly elastic-perfectly plastic in the initial stage of yielding. Divinycell H250 was fully characterized under multiaxial states of stress in the 1-3 plane. A number of tests were conducted to define a failure surface for the material. Experimental results conformed well with the Tsai-Wu failure criterion for anisotropic materials. The most critical region for the material is the compression-compression quadrant. The most critical combination is compression and shear. For more details about the mechanical characterization of facing and core materials refer to references [16] and [17].

The carbon/epoxy facings were bonded to the Divinycell core with an epoxy adhesive (Hysol EA 9430). The assembly was cured at room temperature. The facings and core had a thickness of 1 and 25.4 mm, respectively. Beam specimens 25.4 mm wide and of various lengths were cut from the sandwich plates.

3   Experimental procedure

Special test fixtures were fabricated to provide three- and four-point bending for beams of various lengths. Five span lengths were selected for beams under three-point bending, 10.2, 20.3, 25.4, 40.6 and 76.2 cm. In the four-point bending configuration the distance between supports was 41 cm and the distance between the middle loads was 18 cm. In studying the effects of pure bending, special reinforcement was provided for the core at the outer sections of the beam to prevent premature core failures. Also, under three-point bending, the faces directly under concentrated loads were reinforced with additional layers of carbon/epoxy to suppress and prevent indentation failure. Only in the case when the indentation failure mode was studied, there was no face reinforcement.

Strains on the outer and inner (interface between facing and core) surfaces of the facings were recorded with strain gages. Most gages were oriented along the axis of the beam, but some were mounted in the transverse direction to record transverse strains. Beam deflections were measured with a displacement transducer (LVDT) and by monitoring the crosshead motion. The deflection was also monitored with a course moiré grating (31 lines/cm). Longitudinal and transverse strains in the core were measured with finer moiré gratings of 118 and 200 lines/cm. The deformation of the core was also monitored with birefringent coatings using reflection photoelasticity.

4   Failure modes

A number of failure modes were recorded and studied in the composite sandwich beams subjected to three- and four-point bending. They include wrinkling of the compression facing, core failure and indentation of the loaded face. These failure modes are discussed in the following sections.

4.1   Compression facing wrinkling

Compression facing wrinkling failures were observed in sandwich beams under both four-point and three-point bending. Figure 1 shows moment versus strain results for two different tests of sandwich beams with Divinycell H100 cores under four-point bending. Evidence of wrinkling is shown by the sharp change in recorded strain on the compression facing, indicating inward and outward wrinkling in the two tests. In both cases the critical wrinkling stress was
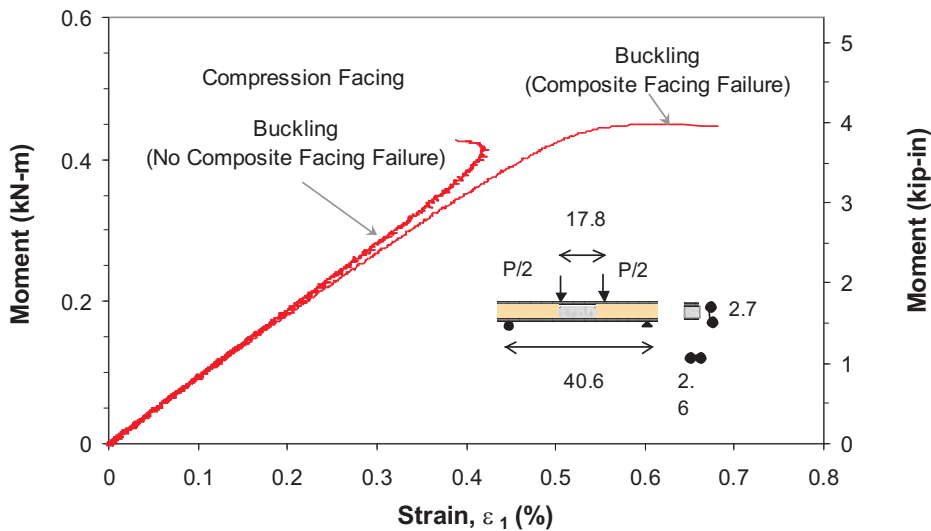
$$\sigma_{cr} = 673 \ MPa$$

Figure 1: Facing wrinkling in sandwich beam under four-point bending Divinycell H100 foam core; dimensions are in *cm*.

Wrinkling is a localized short-wave buckling of the compression facing. Wrinkling may be viewed as buckling of the compression facing supported by an elastic continuum, the core [7]. The critical wrinkling stress according to

Heath [18] is given by

$$\sigma_{cr} = \left[\frac{2}{3}\,\frac{h_f}{h_c}\,\frac{E_{c3}\,E_{f1}}{(1-\,\nu_{12}\,\nu_{21})}\right]^{12} \tag{1}$$

where

h_f, h_c : facing and core thicknesses, respectively

E_{f1}, E_{c3} : facing and core moduli, respectively

ν_{ij} : Poisson's ratio associated with loading in the i-direction and strain in the j-direction

and the indices 1 and 3 refer to the in-plane and through-the-thickness directions, respectively.

Equation (1) predicts the following value of the wrinkling stress

$$\sigma_{cr} = \,687\,MPa$$

This value is close to the experimental value of 673 MPa.

In the case when shear is present in addition to bending, the influence of the transverse shear modulus of the core, G_{c13}, must be taken into account. An early expression given by Hoff and Mautner [7] has the form

$$\sigma_{cr} = \,c\,(E_{f1}\,E_{c3}\,G_{c13})^{1/3} \tag{2}$$

where c is a constant usually taken as equal to 0.5, 0.6, or 0.65. Note that the critical stress in this expression depends only on the elastic moduli of the facing and core materials. In the relation above the core moduli are the initial elastic moduli if wrinkling occurs while the core is still in the linear elastic range. This requires that the shear force at the time of wrinkling be low enough or, at least,

$$V \,<\, A_c\,F_{cs}, \tag{3}$$

where A_c is core cross sectional area and F_{cs} the shear strength of the core. This is the case for long span beams under three-point bending.

In the case of shorter beams where the shear loading component is significant, core failure precedes facing wrinkling. Core yielding and stiffness loss reduce core support of the facings and precipitate facing wrinkling failure at a lower stress. The critical wrinkling stress in that case would be

$$\sigma_{cr} = \,0.5\,(E_{f1}\,E'_{c3}\,G'_{c13})^{1/3} \tag{4}$$

where E'_{c3}, G'_{c13} are the reduced core Young's and shear moduli in the through-the-thickness direction.

Figure 2 shows moment versus strain curves for a 38 cm long beam with Divinycell H250 core under three-point bending. Facing wrinkling seems to

occur at a local bending moment of 330 Nm and a shear force of 2875 N. Introducing a modulus reduction ratio for Young's and shear moduli of

$$\rho_E = \frac{E'_{c3}}{E_{c3}} = \frac{G'_{c13}}{G_{c13}} = 0.385$$

eq.(4) predicts a local critical facing stress equal to the measured value of
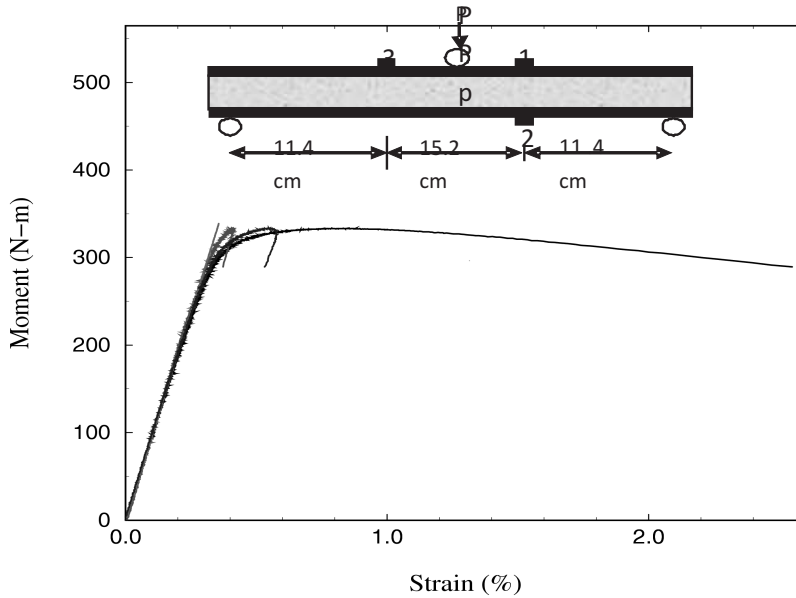
$$\sigma_{cr} = 500\,MPa$$

Figure 2: Moment vs strain curves for sandwich beam under three-point bending. Dimensions are in *cm*.

This reduction (in secant or tangent modulus) is quite possible in view of the high shear strain in the core (over 15% as measured by the photoelastic coating method) and the elastoplastic shear behavior of the core material.

4.2   Core failure

Core failures were observed in sandwich beams under three-point bending. The core carries primarily the applied shear loading. In short beams under three-point bending the core is mainly subjected to shear and failure occurs when the maximum shear stress reaches the critical value (shear strength) of

the core material. In long-span beams the normal stresses in the core become of the same order of magnitude or even higher than the shear stresses. In this case, the core is subjected to a biaxial state of stress and fails according to an appropriate failure criterion. It was shown that failure of the PVC foam core Divinycell H250 can be described by the Tsai-Wu failure criterion [17]. This criterion for a two-dimensional state of stress on the 1-3 plane is expressed as

$$f_1\,\sigma_1 + \ f_3\,\sigma_3 + f_{11}\,\sigma_1^2 + \ f_{33}\,\sigma_3^2 + \ 2f_{13}\,\sigma_1\,\sigma_3 = \ 1 - k^2 \qquad (5)$$

where

$$f_1 = \ \tfrac{1}{F_{1t}} - \tfrac{1}{F_{1c}} \quad , \quad f_3 = \ \tfrac{1}{F_{3t}} - \tfrac{1}{F_{3c}}$$

$$f_{11} = \ \tfrac{1}{F_{1t}\,F_{1c}} \qquad , \quad f_{33} = \ \tfrac{1}{F_{3t}\,F_{3c}} \qquad (6)$$

$$f_{13} = \ - \tfrac{1}{2}\,(f_{11}\,f_{33})^{1/2}$$

$$k = \ \tfrac{\tau_{13}}{F_{13}} = \ \tfrac{\tau_5}{F_5}$$

In the above equations σ_1, σ_3 *and* τ_5 are the normal and shear stresses referred to the principal material directions (in-plane is direction 1 and through-the-thickness is direction 3), F_{1c} and F_{1t} are the compressive and tensile strengths along the in-plane direction, F_{3c} *and* F_{3t} are the compressive and tensile strengths along the through-the-thickness direction and F_5 ($= F_{13}$) is the shear strength on the 1-3 plane.

The state of deformation and failure mechanisms in the core were studied by means of moiré and birefringent coating methods. Figure 3 shows moiré fringe patterns in the core of a sandwich beam with Divinycell H250 core under three-point bending. The moiré fringe patterns corresponding to the horizontal and vertical displacements away from the applied load consist of nearly parallel and equidistant fringes from which it follows that the normal strains are zero, while the shear strain is nearly constant across the core thickness. This is valid only in the linear range. In the nonlinear and plastic region the core begins to yield. The shear stress distribution in the core was monitored with birefringent coatings of 0.5 and 1 *mm* thickness (PS-4D coatings, Measurement Group). The coating is bonded to the surface of the core with a reflective cement to insure light reflection at the interface. A still camera and a digital camcorder were used to record moiré and isochromatic fringe patterns. From the isochromatic fringe patterns it was shown that, after the linear elastic region of Divinycell H250 is exceeded, the shear strain becomes highly nonuniform across the core thickness peaking at the center. It was found that the shear deformation starts becoming nonuniform at an applied load of 3.29 kN which corresponds to an average shear stress of 2.55 MPa. This is close to the proportional limit of the shear strain-strain curve of Divinycell H250.

As the load increases beyond this point the shear strain in the core becomes nonuniform peaking at the center.
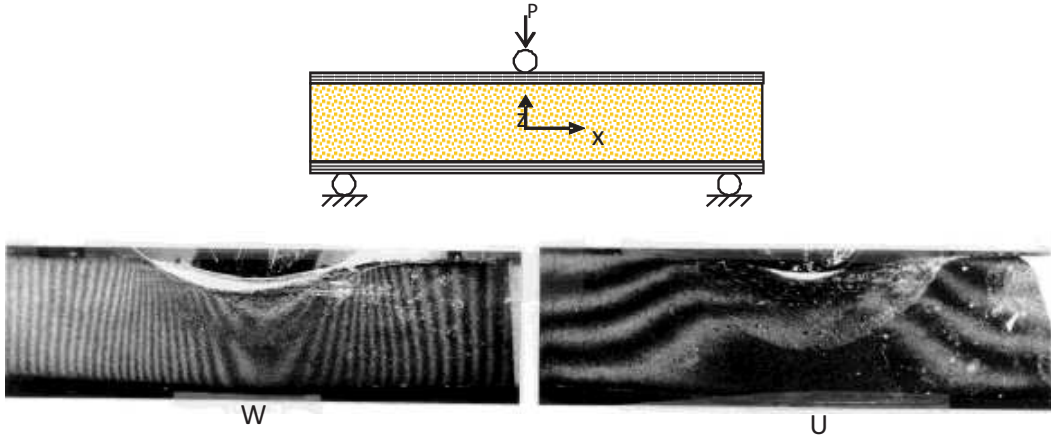

Figure 3: Moiré fringe patterns corresponding to horizontal and vertical displacements in sandwich beam under three-point bending (12 lines/mm; Divinycell H250 core).

4.3   Indentation failure

Indentation failure was observed in beams under three-point bending when no special reinforcement of the facing or the core was provided in the area under the load. Figure 4 shows the variation of the applied load with the displacement of the indenting roller for a 36 cm long beam under three-point bending. The displacement represents the sum of the global beam deflection and the local indentation, but it is more sensitive to the local indentation. Therefore, the proportional limit of the load-displacement curve is a good indication of initiation of indentation. In the present case the beam was made with a Divinycell H100 core. The load at initiation of indentation is 735 N. The peak load measured was P_{max}= 1080 N. Figure 5 shows moiré fringe patterns corresponding to vertical displacements for a beam in three-point bending. It shows the development of indentation and the area of the beam affected by the indentation.

   The indentation failure of the sandwich beam can be predicted by treating the loaded face as a beam resting on a foundation. For linear elastic behavior, the core is modeled as continuous distributed linear tension/compression springs. The stress σ at the interface between core and facing is proportional to the local deflection, w
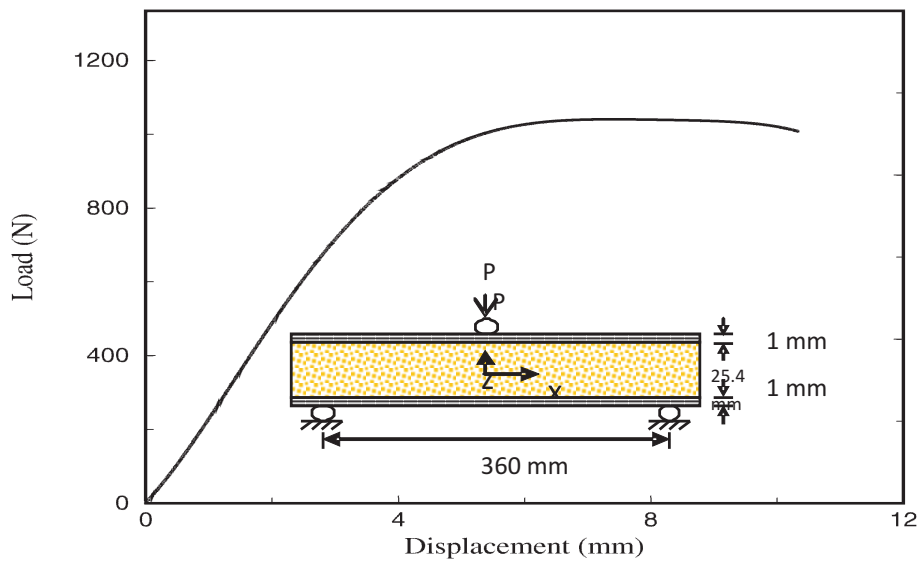
$$\sigma = kw \qquad (7)$$

Figure 4: Load versus deflection under load of sandwich beam under three-point bending (carbon/epoxy facings, Divinycell H100 core).
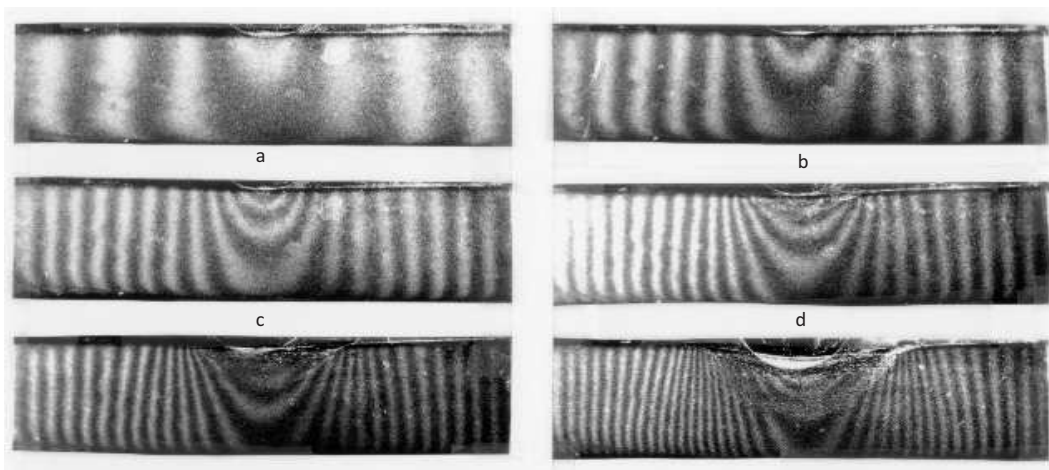

Figure 5: Moiré fringe patterns in sandwich beam with foam core corresponding to vertical displacements at various applied loads (12 lines/mm grating). Loads: (a) 318 N, (b) 574 N, (c) 812 N, (d) 924 N, (e) 1057 N, (f) 1080 N

where k is the foundation modulus given by [19]

$$k = 0.64 \frac{E_{c3}}{h_f} \sqrt[3]{\frac{E_{c3}}{E_{f1}}} \tag{8}$$

For a long (assumed infinite) facing the deflection w_P under the load P is

$$w_P = \frac{P\lambda}{2kb} \tag{9}$$

where

$$\lambda = \frac{1.18}{h_f} \sqrt[3]{\frac{E_c}{E_{f1}}} \tag{10}$$

and b is the width of the facing.

Yield of the core under the load occurs when the interfacial stress σ reaches the yield stress of the foam core. The critical load at initiation of core yield is calculated from Eqs.(7) to (10) and the yield condition as

$$P_{cy} = 1.70\,\sigma_{ys}\,b\,h_f \sqrt[3]{\frac{E_{f1}}{E_c}} \tag{11}$$

where σ_{ys} is the yield stress of the core.

As the load increases beyond the yield value, plastic deformation propagates through the core from the center to the ends of the facing. For a rigid-perfectly plastic foundation the local bending stress at the upper surface of the facing is given by [13]

$$\sigma_{fl} = \frac{9\,P^2}{16\,b^2\,h_f^2\,\sigma_{ys}} \tag{12}$$

For a beam in three-point bending the global stress in the facing is

$$\sigma_{fb} = \frac{PL}{4\,b\,h_f\,(h_f + h_c)} \tag{13}$$

where h_c is the thickness of the facing.

Indentation failure occurs when the sum of the local and global bending stresses, σ_{fl} and σ_{fb}, reaches the compressive strength of the facing material.

The load at initiation of indentation in Figure 4 is 735 N and agrees with the calculated value of 800 N from Eq. (11). The peak load measured is $P_{max} = 1080$, while the calculated value is $P_{max} = 1310\,N$. The difference in the results may be attributed in the simplifying assumption of a rigid-perfectly plastic foundation.

5   Failure mode transition

From the above discussion it is obvious that initiation of a particular failure mode depends on the geometrical characteristics, the material properties and the loading conditions of the beam. In the case of beams under three-point bending when reinforcement of the facings or the core is provided to suppress indentation failure, the prevalent failure modes are facing wrinkling and core failure. For short spans, core failure occurs first and then it triggers facing wrinkling. For long spans, facing wrinkling can occur before any core failure. Core failure initiation can be described by calculating the state of stress in the core and applying the Tsai-Wu failure criterion. Thus, a curve for the critical load for core failure initiation versus span length is obtained. On the other hand, the critical load for facing wrinkling as a function of span length can be predicted from Eq. (2). Figure 6 shows curves of the critical load versus span length for initiation of failure by core failure and facing wrinkling for a sandwich beam with Divinycell H250 foam core. The intersection of the curves defines the transition from core failure initiation to facing wrinkling initiation. The span length for failure mode transition for the beam materials and cross section considered is L = 35 cm.
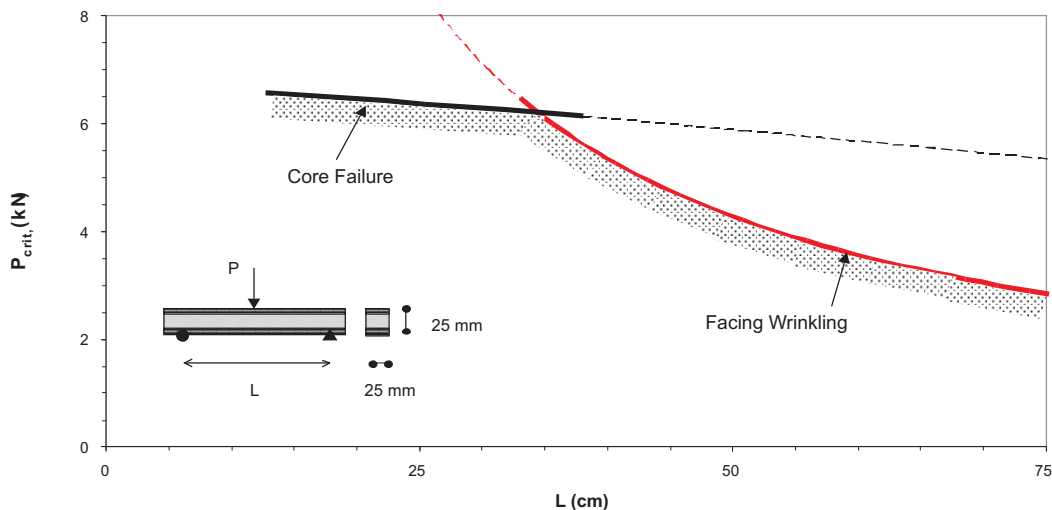

Figure 6: Critical load versus span length for failure initiation in sandwich beams under three-point bending.

6   Conclusions

Failure modes of composite sandwich beams depend on the type of loading, constituent material properties and geometrical dimensions. For sandwich beams made of unidirectional carbon/epoxy facings and PVC closed-cell foam cores failure modes observed and studied include core failure, compressive facing wrinkling and indentation failure. Experimental results were compared with theoretical predictions whenever they were available. Following initiation, interaction of failure modes takes place leading to catastrophic fracture. Thus, failure initiation by plastic deformation of the core degrades the supporting role of the core and precipitates other failure modes, such as facing wrinkling. When core failure and stiffness degradation occur first, the critical wrinkling stress is substantially reduced. Thus, catastrophic failure of a sandwich beam appears to be the result of initiation/propagation and interaction of failure modes, as influenced by type of loading, constituent material properties and geometrical dimensions.

References

[1] I.M. Daniel, E.E. Gdoutos, K.-A. Wang, and J.L. Abot, Failure modes of composite sandwich beams, Int. J. Damage Mech., 11, (2002), 309-334.

[2] H.G. Allen, Analysis and design of structural sandwich panels, Pergamon, London, 1969.

[3] D.J. Hall and B.L. Robson, A review of the design and materials evaluation programme for the GRP/foam sandwich composite hull of the RAN minehunter, Composites, 15, (1984), 266-276.

[4] D. Zenkert, An introduction to sandwich construction, Chameleon, London, 1995.

[5] I.M. Daniel, J.L. Abot, and K.-A. Wang, Testing and analysis of composite sandwich beams, Proc. of ICCM 12, Paris, France, 1999.

[6] I.M. Daniel, and J.L. Abot, Fabrication testing and analysis of composite sandwich beams, Comp. Sci. Tech., 60, (2000), 2455-2463.

[7] N. J. Hoff, and S.E. Mautner, The buckling of sandwich-type problems, J. Aero. Sci., 12 (1945), 285-297.

[8] A.J. Gutierrez, and J.P.H. Webber, Flexural wrinkling of honeycomb sandwich beams with laminated faces, Int. J. Sol. Struct., 16, (1980), 645-651.

[9] W.K. Vonach, and F.G. Rammerstorfer, Wrinkling of thick orthotropic sandwich plates under general loading conditions, Arch. Appl. Mech., 70, (2000), 338-348.

[10] B.K. Hadi and F.L. Matthews, Development of Benson-Mayers theory on the wrinkling of anisotropic sandwich panels, Comp. Struct., 49, (2000), 425-434.

[11] T.C. Triantafillou and L.J. Gibson, Debonding in foam-core sandwich panels, Mat. Struct., 22, (1989), 64-69.

[12] J.L. Avery III, and B.V. Sankar, Compressive failure of sandwich beams with debonded face sheets, J. Comp. Mat., 34, (2000), 1176-1199.

[13] P.D. Soden, Indentation of composite sandwich beams, J. Strain Anal., 31, (1996), 353-360.

[14] Schuaeib, F. M. and P.D. Soden, Indentation failure of composite sandwich beams, Comp. Sci. Tech., 57, (1977), 1249-1259.

[15] T.C. Triantafillou and L.J. Gibson, Failure mode maps for foam core sandwich beams, Mat. Sci. Engng., 95, (1987), 37-53.

[16] E.E. Gdoutos, I.M. Daniel, K.-A. Wang, and J.L. Abot, Nonlinear behavior of composite sandwich beams in three point bending, Exp. Mech., 41, (2001), 182-188.

[17] E.E. Gdoutos, I.M. Daniel, and K.-A. Wang, Failure of cellular foams under multiaxial loading, Composites-Part A, 33, (2002), 163-176.

[18] W.G. Heath, Sandwich construction, Part 2: The optimum design of flat sandwich panels, Aircraft Engng., 32, (1960), 230-235.

[19] M. Hetenyi, Beams on elastic foundation, The University of Michigan Press, 1946.

Modovi otkaza kompozitnih greda strukture sendviča

U radu je prikazano detaljno istraživanje grede od kompozitnog sendvič materijala opterećenog na savijanje jednomn ili sa dve koncentrisane sile. Grede su izradjene od pravolinijskih grafitnih/epksi lamela i PVC zatvorenih čelija pletiva. Konstitutivni materijali su potpuno opisani i u slučaju pletiva, anvelope rušenja su konstruisane za opšte dvodimenzionalno stanje napona. Različiti modeli rušenja uključujući listanje (boranje), degradacija probojem i globalna destrukcija nosaǎ su uočeni i uporedjeni sa analitičkim postupkom. Početak, propagacija i interakcija modova rušenja zavise od tipa opterećenja, konstiutivnih materijala i geometrije nosača.